sciendo

Polish Journal of Chemical Technology, 24, 2, 50—56, 10.2478/pjct-2022-0014

High performance fluidized bed photoreactor for ethylene decomposition

Piotr Rychtowski, Piotr Miądlicki, Bartłomiej Prowans, Beata Tryba*

West Pomeranian University of Technology in Szczecin, Faculty of Chemical Technology and Engineering, Department of Catalytic and Sorbent Materials Engineering, Pułaskiego 10, PL 70-322 Szczecin, Poland.
**Corresponding author: e-mail: beata.tryba@zut.edu.pl*

Removal of C_2H_4 in the air was carried out in the continuous flow reactor with the photocatalytic bed (expanded polystyrene spheres coated by TiO_2 or SiO_2/TiO_2) under irradiation of UV light. Continuous flow of a gas stream through the reactor was realised at the static bed and under bed fluidization. The required flow of a gas stream through the reactor for bed fluidisation was 500–700 ml/min, whereas for the static bed the flow rate of 20 ml/min was used. Fluidized bed reactor appeared to be much more efficient in ethylene removal than that with the stationary bed. It was caused by the increased speed of C_2H_4 mass transfer to the photocatalyst surface and better utilization of the incident UV light. In the fluidized bed reactor calculated rate of C_2H_4 degradation was around 10 μg/min whereas in the stationary state 1.2 μg/min only.

Keywords: ethylene degradation, photocatalytic bed reactor, fluidization, TiO_2.

INTRODUCTION

Ethylene in the natural environment occurs in a gas form, and it is a plant hormone produced across fruits and vegetables. There is observed both, the positive and harmful incomings of ethylene in the agricultural industry. As positive effect ethylene can accelerate maturation of plants, but on the other side is responsible for aging of vegetables and fruits, worsen of their physical parameters and faster spoiling[1]. The harmful effect of ethylene appears after harvesting when the fruits and vegetables are shipped or transported by trucks and storage[2]. There are some classical methods used to reduce the concentration of ethylene in a storage atmosphere, such as ventilation, adsorption, potassium permanganate oxidation, catalytic oxidation or exposure to ozone. Recently photocatalytic methods of removal ethylene from the atmosphere are studied. The most commonly used material as a photocatalyst is titanium dioxide in the form of anatase phase[3–5].

Photocatalytic decomposition of ethylene on illuminated TiO_2 surface depends on the physicochemical parameters of the photocatalytic material and operational conditions of a process. For the photocatalytic tests, TiO_2 material is often immobilized on different types of supports, such as glass, alumina, silica, activated carbon, polymers or others[1–9]. The photocatalytic process of ethylene removal can be carried out in the reactors with fixed TiO_2 on the reactor walls or with supported TiO_2 on different material as the stationary or mobile bed. High efficiency of ethylene degradation can be achieved for high developed surface of the photocatalytic material and its good interaction with the ethylene molecules. In the mechanism of ethylene decomposition hydroxyl radicals formed upon TiO_2 excitation take an important role. It was reported, that TiO_2 with high hydroxylation surface was efficient for the oxidation of ethylene[1, 5, 10–12]. Ethylene is poorly adsorbed on TiO_2, but its interaction with titania surface increases, when TiO_2 is irradiated with UV irradiation[5, 12]. Decomposition of C_2H_4 proceeds through its conversion to formaldehyde and formic acid with the following mineralisation to CO_2 and H_2O. For total mineralisation of 1 mol of C_2H_4, 12 mols of hydroxyl radicals are utilized, according to the reaction:

$$C_2H_4 + 12\ OH^{\bullet} \rightarrow 2\ CO_2 + 8\ H_2O \qquad (1)$$

Hydroxyl radicals can be formed by the reaction of photoinduced holes with hydroxyl ions or via reduction of H_2O_2 through photoinduced electrons or anionic peroxide radicals[13], as it was illustrated in reactions (2–4):

$$HO^- + h^+ \rightarrow HO^{\bullet} \qquad (2)$$

$$H_2O_2 + e^- \rightarrow HO^{\bullet} + HO^- \qquad (3)$$

$$H_2O_2 + O_2^{-\bullet} \rightarrow HO^{\bullet} + HO^- + O_2 \qquad (4)$$

Hydrogen peroxide forms on the illuminated TiO_2 surface during photocatalytic chain reactions occurring with the reactive radicals.

Considering this, C_2H_4 decomposition will be depended on the photocatalytic properties of TiO_2 such as ability to generation of reactive radicals and good separation of free charges. Fast diffusion of C_2H_4 molecules to the titania surface will be essential together with obtaining a high yield of incident photons absorption during UV irradiation of TiO_2. Therefore the proper design of the photocatalytic system is very important. In the continuous flow photoreactors with the stationary bed, low velocity of a gas flow such as 2.5–20 ml/min is usually applied[4, 5, 8], what gives good conditions for the mass transfer of C_2H_4 to the photocatalytic surface. In batch type reactors, usually, a fan is mounted inside with air circulation, then diffusion of C_2H_4 to the active surface of TiO_2 is boosted by a speed of air blowing. However, to achieve bed fluidization, higher velocity of a gas stream flowing through the reactor is necessary, it varies depending on the porosity, size and density of a bed, diameter of the reactor and the height of the fluidized bed[14]. In the reported studies on the removal of ethylene in the fluidized bed (TiO_2 supported on the alumina microspheres), the applied velocity of a gas stream was 80 dm^3/min[8]. In the other studies, some researchers conducted the removal of gaseous toluene in a fluidized bed reactor and used as a bed activated carbon (AC) with supported TiO_2. They proved, that deduction of toluene in a flowing gas stream was mass transfer limited reaction and the highest yield was achieved for the enrichment of toluene concentration on the photocatalyst surface. They used the flow rate of a gas stream in the range of 3–20 dm^3/min[15]. Another important parameter in a fluidized bed photoreactor is light scattering of the incident light. In order to increase light scattering in the fluidized bed (AC/TiO_2) some researchers added SiO_2 and obtained

increased efficiency of the photocatalytic reactions[15]. The quantity of the fluidized bed should be optimally designed in order to avoid light shielding. The photocatalytic process in the fluidized bed reactor should be carried out with the velocity of gas flow much higher than the minimum fluidization velocity (MFV). For the photocatalytic degradation of trichloroethylene in the fluidized bed reactor (TiO_2/silica gel) the highest efficiency was achieved, when the velocity of a gas flow was three times higher than MFV, where MFV was estimated to be 640 ml/min[16]. The lower velocity of a gas flow caused light shielding but for higher one, the efficiency was rate limited reaction occurring on TiO_2 surface[16]. The source of the light, power and way of irradiation are essential for the efficacy of the photocatalytic reactions. In the reported schemes of the photocatalytic reactors generally the source of lamp was usually placed inside or outside of the reactor chamber, the distance between the lamp and photocatalyst was important and should be considered during reactor design process, because higher power of UV light generates higher yield of the photocatalytic reactions. By approaching the source of lamp to the photocatalyst bed there is a high increase of energy flux in the reaction chamber. Therefore both, the amount of the photocatalyst and quantity of the absorbed photons are important in the yield of the photocatalytic process. In this paper photocatalytic degradation of C_2H_4 was conducted in the fluidized bed reactor under the conditions of the stationary and mobile bed. A comparison of the C_2H_4 removal from the gas stream was performed, taking into account the stationary and mobile bed together with the type and amount of TiO_2 immobilized on the EPS support.

EXPERIMENTAL

Expanded polystyrene spheres (EPS) were coated by TiO_2 or SiO_2/TiO_2 bilayer in two steps. Two titania materials were used for coating, nanocrystalline TiO_2 of anatase phase obtained in the laboratory and commercial titania P25 produced by Evonik Company (Germany), which was a mixed structure of anatase and rutile in the ratio of 78:22, respectively. TiO_2 prepared in the laboratory was obtained by the hydrothermal treatment of an amorphous hydrolyzed titania in an autoclave at 150 °C under the pressure of 7.4 bar for 1 hour, followed by the thermal treatment at 400 °C under flow of Ar. The hydrolyzed titania was a semiproduct obtained from the production of the titania white in Police Chemical Factory (Poland) through the sulfuric method. Such prepared sample was selected for EPS coating, based on the previous studies on the ethylene decomposition on TiO_2 reported elsewhere[5].

The phase composition and crystallinity of TiO_2 and SiO_2 materials were determined by XRD technique. XRD measurements were performed using Empyrean diffractometer (Malvern PANanalytical Ltd. company, Almelo, Netherlands) with the utilization of a Cu lamp (λ = 0.154439 nm). The measurements were performed with set up parameters of Cu lamp 30 mA and 35 kV. The mean size of rutile and anatase crystallites were calculated from the Scherrer equation and by the use of Rietveld method.

The porosity of TiO_2 samples was determined through the measurements of nitrogen adsorption at low temperature in QUADRASORB Si analyzer (Quantachrome, Boynton Beach, FL, USA). Before measurement, all the samples were degassed at 150 °C for 12 h under high vacuum using MasterPrep degasser. Specific surface areas (SSA) of the studied samples were calculated on the basis of the obtained nitrogen adsorption isotherms by using BET method.

The electrokinetic potential of the titania surface was determined in Zetasizer Nano ZS apparatus. These measurements were performed in order to analyze the affinity of TiO_2 surface to the SiO_2. Analyzed TiO_2 samples were suspended in ultrapure water. The suspension was prepared by mixing 5 mg of photocatalyst and 100 ml of ultrapure water, followed by 30 minutes of magnetic stirring.

Thermogravimetric analyses were applied to determine the quantity of hydroxyl groups in the titania samples. This technique was also used to analyze the silica and titania content in P-TiO_2 and P-SiO_2-TiO_2 composites. All the measurements were carried out under the nitrogen flow (99.999% pure, 30 ml/min) in the thermobalance (Netzsch STA 449 C, Germany). Temperature program, which was set up to analyze the quantity of OH groups was as follows: heating to 120 °C with 30-minute isothermal step, then heating to 500 °C with 15-minute isothermal step. This procedure was elaborated based on the earlier experiments and other literature dispatch[5, 17, 18]. The contents of silica and TiO_2 in the P-TiO_2 and P-SiO_2-TiO_2 composites were calculated from the mass loss of EPS coated spheres after their heating up to 600 °C with the heating rate of 20 K/min. The sample weight used for analyses was approximately 10 mg.

EPS coating by silica layer was carried out via Stöber method[19]. Simply 0.8 g of φ1 mm EPS spheres were mixed with 60 ml of EtOH and 1.5 ml of 30% ammonia solution, followed by 30 minutes stirring at ambient temperature. Afterwards, 30 ml of ethanol with 2 g of tetraethyl orthosilicate were added drop by drop. The obtained mixture was stirred for 24 h, followed by processing in rotary evaporator until full solvent evaporation occurred. Obtained P-SiO_2 composites were dried at 70 °C for 24h.

In the second approach for P-SiO_2 preparation, simple mixing of commercial SiO_2 nanopowder (Aerosil® OX50) used in excess with 1g of EPS was realized. This mixture was then heated in oven at 140 °C for 24 h. Obtained composites were separated from the remaining silica on the φ0.2 mm mesh size sieve. In the second step, P-SiO_2 composites were coated with TiO_2 from the titania slurry solution. Titania coating was carried out in the rotary evaporator under high vacuum, until full water evaporation occurred. This process was carried out twice in order to obtain better TiO_2 coatings.

The morphology of the samples was analyzed by FE-SEM in SEM Hitachi SU8020 with field cold emission.

The photocatalytic decomposition of ethylene was carried out in the quartz tube (φ10 mm), where gas mixture was entered from the bottom of the reactor. The initial height of 8 cm of EPS composites was used as the photocatalytic bed. Measurements were performed in two conditions: stationary and under bed fluidization.

Stationary bed measurements were conducted at the flow rate of 20 ml/min, whereas fluidized bed measurements at the flow of either 500 or 700 ml/min, in order to obtain fluidization height of 13 cm. The model ethylene gas mixture of 50 ppm in the synthetic air was supplied to the photoreactor from the bottle. The photocatalytic tests in the photoreactor were carried out at room temperature and in the presence of light emitted by 3 ring shaped UV lamps (Philips, Eindhoven, The Netherlands, Special 'TL'E 22W/10 Black Light). The scheme of the photocatalytic system was introduced in Fig. 1, and in Fig. 2 emission spectrum of these UV lamps was added.

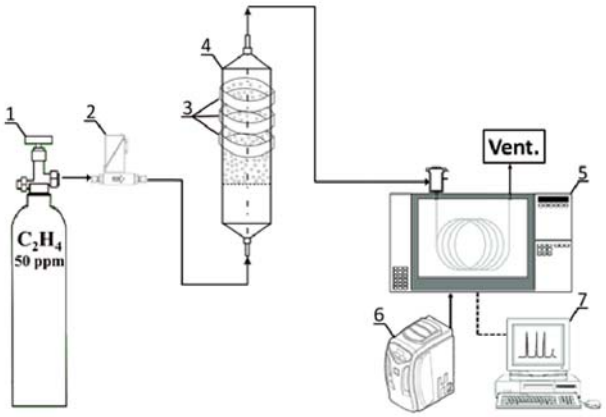

Figure 1. The scheme of the photocatalytic system: 1 – bottle of synthetic air with ethylene gas (50 ppm), 2 – flow meter, 3 UV lamps, 4 – quartz photoreactor φ10 mm with stationary/fluidized bed of P-SiO_2-TiO_2 composites, 5 – gas chromatograph SRI 8610C with FID detector, 6 – hydrogen generator, 7 – Personal Computer

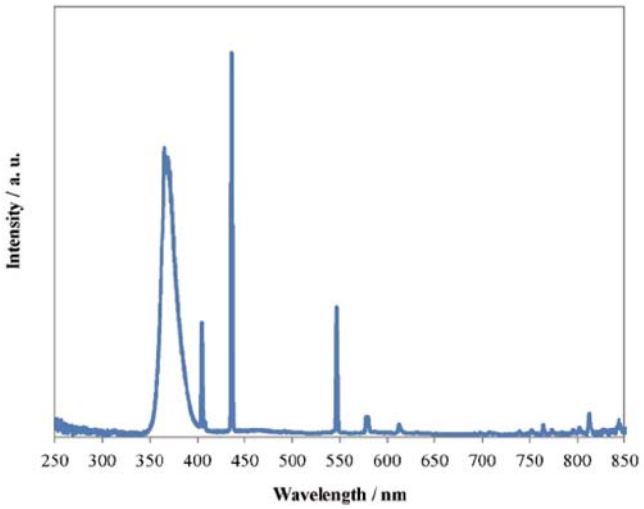

Figure 2. The emission spectrum of UV lamps

The measurements of incident UV light on the reactor walls were performed by using LB-901 arrangement with PD204 light sensor for the wavelength range of UVA and UVB (Macam Photometrics Ltd.). These measurements were carried out for the emitted light coming through the quartz walls of empty reactor, and then coming through the photocatalytic bed at the stationary conditions and under bed fluidization. In Fig. 3 there are illustrations of the fluidized bed reactor with the indications of the measurements points of a sensor together with the obtained results of radiation intensities.

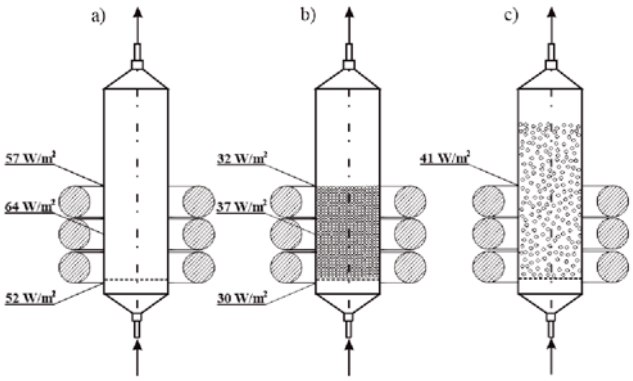

Figure 3. The scheme of the fluidized bed reactor with the measurements points of the incident UV light intensity for: a) an empty reactor, b) reactor with the stationary bed, c) reactor with the fluidized bed

The highest irradiation intensity (64 W/m^2) was noted at the middle point of UV lamps set. The light intensity was somewhat lower at the top and bottom of this UV lamps set. The shielding effect of the photocatalytic bed under the stationary conditions was around 42–44%, whereas under fluidization 28%.

RESULTS AND DISCUSSION

In Fig. 4 there are presented XRD patterns of silica obtained through the sol-gel method and TiO_2 samples used for coating. Wide and low intensity peak in the silica X-ray pattern was referred to the amorphous form of SiO_2. Both TiO_2 samples indicated mixed anatase and rutile phases, however, for commercial P25 the intensity of rutile reflex was higher than for Ar400. All the peaks in the X-ray pattern of P25 were more intensive and narrow in comparison with those obtained for Ar400, so the commercial TiO_2 presented higher crystallinity. In Table 1 there are presented the physicochemical characteristics of titania samples used in these studies.

TiO_2 prepared in the laboratory consisted mostly from nanocrystalline anatase, exhibited high BET surface area and quite large hydroxylation of surface by comparison with commercial P25. The commercial titania was a mixture of anatase and rutile in the ratio of 78:22, respectively, represented 3 times lower surface area than the laboratory TiO_2 sample and had higher

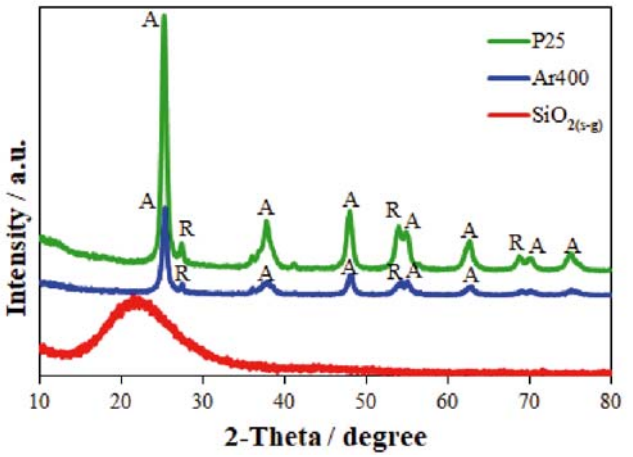

Figure 4. XRD patterns of studied TiO_2 samples and SiO_2 obtained through the sol-gel process

Table 1. The physicochemical properties of TiO_2 samples

Sample name	BET surface area (m^2/g)	Phase composition (%)	Average crystallites size (nm)	OH groups (wt%)	Zeta potential (mV)
P25	54	Anatase: 78 Rutile: 22	Anatase: 21 Rutile: 55	1.0	+31.0 at pH = 5.4
Ar400	167	Anatase: 97 Rutile: 3	Anatase: 15 Rutile: 95	4.1	+13.0 at pH = 6.7

value of electrokinetic potential. It is worth to notice, that P25 exhibited higher acidic character than Ar400, because, during measurements zeta potential in the ultra-pure water pH was dropped to 5.4 in the case of P25 sample, whereas for the laboratory made sample was little changed, dropped down to 6.7. Preparation of TiO_2 sample at low temperature such as 400 °C did not allow to its complete crystallization, therefore this sample contained much more OH groups than crystalline P25, its crystallinity was around 78%.

In Table 2 there are presented results from TG measurements for coated EPS spheres. SiO_2 obtained in a sol-gel process was marked as SiO_2(s–g) and the powder one as SiO_2(p).

Table 2. TiO_2 and SiO_2 contents based on TG analyses

Sample	SiO_2 [wt%]	TiO_2 [wt%]
P-SiO_2(s-g)	8.2	–
P-SiO_2(p)	3.2	–
P-Ar400	–	27.2
P- P25	–	28.7
P-SiO_2(s-g)-Ar400	8.2	27.2
P-SiO_2(s-g)-P25	8.2	17.6
P-SiO_2(p)-P25	3.2	11.9

In the applied sol-gel process around 8 wt% of SiO_2 was coated EPS spheres, whereas powdered sintering at 140 °C resulted in a thinner layer coating with the quantity of around 3 wt%. Immobilization of TiO_2 on EPS spheres was comparable for both types of TiO_2 used and equaled around 27–29 wt%. More diversified amount of TiO_2 loading was observed in the case of SiO_2/TiO_2 bilayer coating. The quantity of TiO_2 immobilized on P-$SiO_{2(s-g)}$ spheres after sol-gel process differed much between these two TiO_2 samples, for P25 was around 18 wt%, whereas for TiO_2-Ar400 was much higher, 27 wt%. This difference can be explained by the physicochemical parameters of samples, TiO_2 with higher quantity of OH groups and more basic character exhibited higher affinity to the acidic SiO_2 surface. The quantity of P25 coated on P-$SiO_{2(p)}$ spheres obtained through the sintering at 140 °C was much lower than in case of SiO_2 coating performed via a sol-gel method.

SEM measurements were performed to analyze the morphology of the EPS coated spheres. The surface of P-$SiO_{2(s-g)}$-P25 looked more smooth (Fig. 5a–b) than that obtained through the powder sintering (Fig. 5c–d). Moreover, EPS coated SiO_2 from the sol-gel solution and then immobilized with TiO_2 has rather thick shell composed of multilayers, contrary to that, obtained during sintering with SiO_2 nanoparticles. Sintering at 140 °C caused shrinkage of the EPS spheres with reduction of their size around half of the original one. The size of P-$SiO_{2(s-g)}$-P25 was around 1.1 mm (Fig. 5a), whereas those ones obtained through the sintering method was 0.45 mm (Fig. 5c). During heating at 140 °C, the silica particles were molten in EPS structure, some cracked

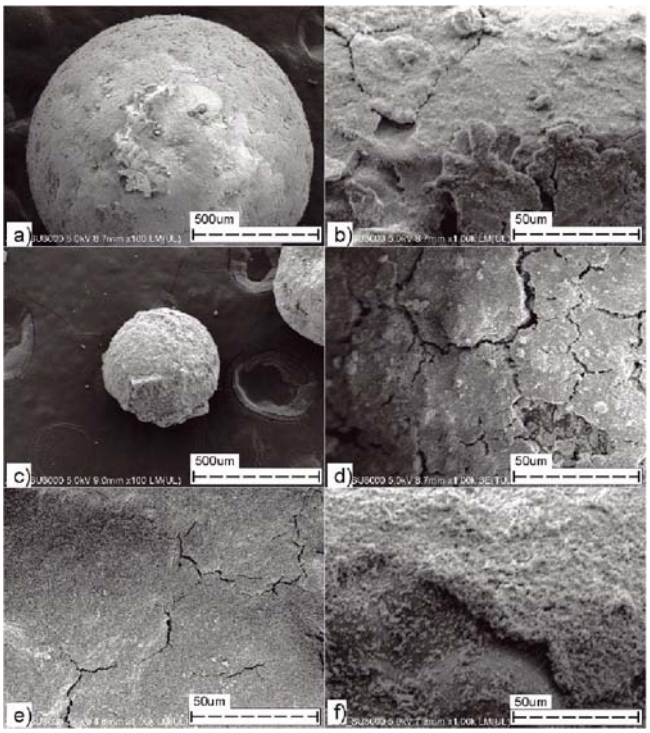

Figure 5. SEM images of EPS coated spheres, a) and b) P--SiO_2(s-g)-P25; c) and d) P-SiO_2(p)-P25; e) P-P25; f) P-Ar400

and molten layers are observed in Fig. 5d. The difference between TiO_2 prepared in the laboratory and commercial P25 can be seen in Fig. 5e-f, more porous structure exhibited sample Ar400 (Fig. 5f). This difference is caused by different preparation methods, Ar400 exhibited more than 3 times higher specific surface area than P25.

The results from the photocatalytic tests performed for ethylene decomposition in the continuous flow reactor with the stationary bed are presented in Fig. 6.

High decomposition of ethylene was achieved on P-TiO_2 and P-SiO_2-TiO_2 spheres in the case of both-TiO_2 samples, with removal efficacy of 50 ppm ethylene within 15 min.

However, the decomposition rate decreased, when silica was coated by sintering with EPS spheres at 140 °C. In fact, P-$SiO_{2(p)}$-P25, which showed low photocatalytic activity contained the lowest quantity of immobilized TiO_2, around 12 wt% only. Obtained results are much better than those reported by the other researchers, which were referred to C_2H_4 decomposition on various supports. For example, C. Maneerat et al.[4] reported decomposition of 10 ppm C_2H_4 in the continuous flow fluidized bed reactor filled with TiO_2 supported on the glass, for the gas flow rate 5 ml/min and UV-A irradiation intensity of 1 mW/cm^2. M. Iwanaga et al. obtained removal of C_2H_4 with concentration of 1 ppm in 22 dm^3 within 60 min on TiO_2 supported glass in the fluidized bed reactor[7]. When TiO_2 was supported on silica, then degradation rate of C_2H_4 under UV irradiation was even less than 1 ppm[6]. De Chiara et al.[8] applied alumina microspheres

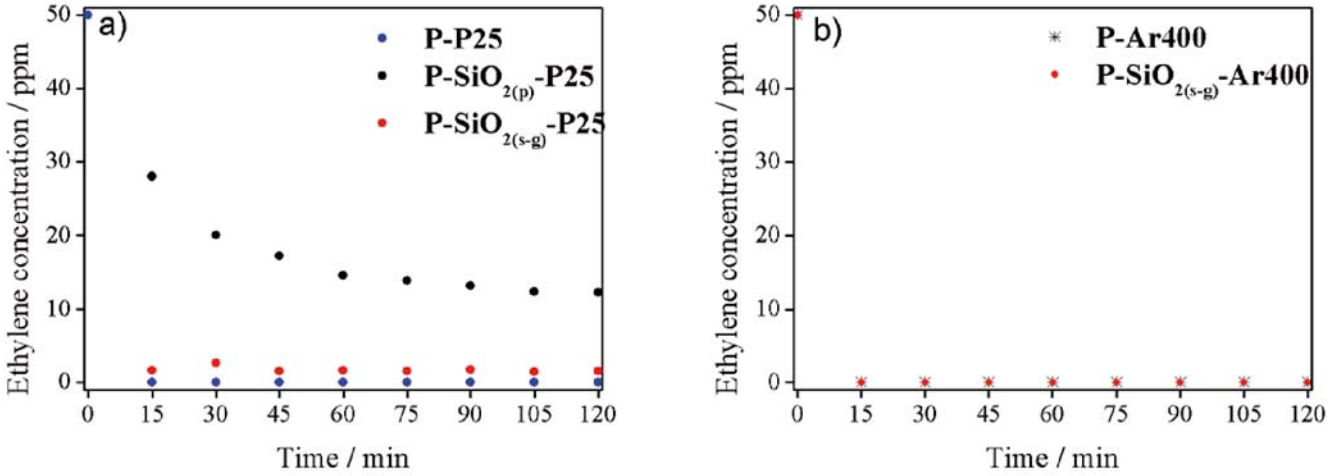

Figure 6. Rate of ethylene decomposition in the photoreactor with the stationary bed for EPS spheres coated with TiO_2 and SiO_2-TiO_2, a) P25; b) Ar400; flow rate: 20 ml/min

coated TiO_2 as a fluidized bed and they obtained 72% reduction of C_2H_4 in a gas stream after 4.5 h for the initial concentration of 40 ppm and power of UV irradiation 36 W. They used reactor with a gas recirculation.

In Fig. 7 there are presented results from the photocatalytic decomposition of ethylene in the fluidized bed reactor under fluidization process.

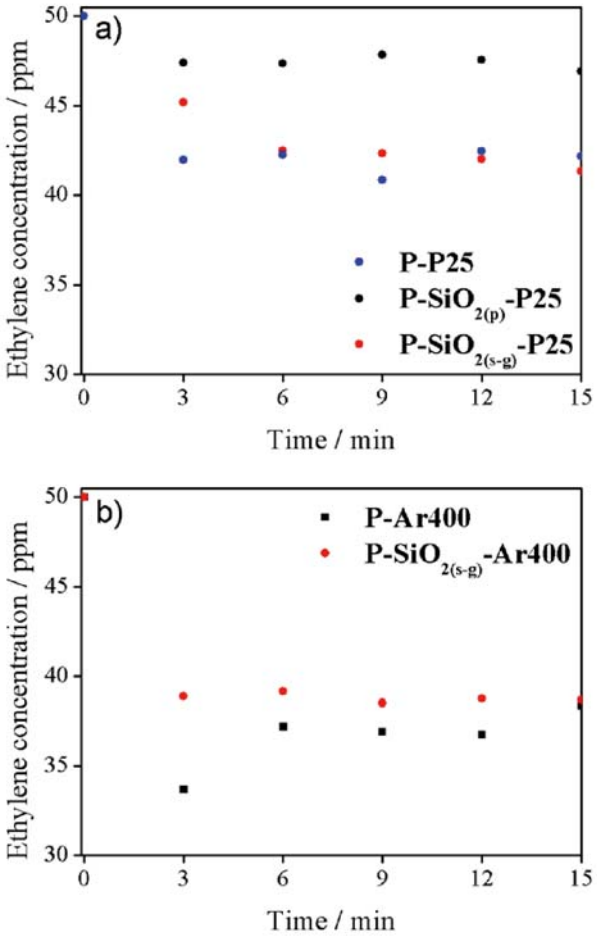

Figure 7. Rate of ethylene decomposition in the photoreactor with the fluidized bed for EPS spheres coated with TiO_2 and SiO_2-TiO_2, a) P25; b) Ar400; flow rate: 500 ml/min and 700 ml for P-SiO_2(p)-P25

The height of the bed in the photoreactor was 8 cm and during fluidization process was extended up to 13 cm. This process requires much higher velocity of gas flow through the bed than in case of the stationary conditions. For EPS spheres coated by TiO_2 or bilayer SiO_2-TiO_2, where SiO_2 was coated via sol-gel process, the velocity of a gas flow was 500 ml/min. The determined minimum fluidization velocity for P-TiO_2 samples was 120–123 ml/min, whereas for P-SiO_2(s-g)-TiO_2 was somewhat higher, 135–140 ml/min. However for P-$SiO_{2(p)}$-P25 the MFV increased significantly and was equaled 270 ml/min. Therefore, for this P-$SiO_{2(p)}$-P25 sample, in order to attain the fluidization of the bed up to height of 13 cm, the velocity of a gas flow through the reactor was 700 ml/min. Higher speed of a gas flow was forced by higher density of P-$SiO_{2(p)}$-P25 spheres, which shrunk after heat-treatment. The measured bulk density of uncoated EPS spheres was 28 kg/m^3, whereas after coating with TiO_2 or bilayer SiO_2/TiO_2 increased slightly up to 30–37 kg/m^3, but thermal treatment at 140 ^{o}C caused dramatic jump of P-$SiO_{2(p)}$-P25 bulk density to 496 kg/m^3.

Higher velocity of a gas flow in the fluidized bed reactor by comparison to that with the stationary bed caused lower rate of ethylene degradation. When we compare two various TiO_2 samples coated EPS spheres with similar quantity, it is clearly observed, that Ar400 was much more effective in ethylene degradation than P25. Laboratory made sample showed decomposition rate of ethylene over 25% in the continuous flow reactor, whereas P25 15% only at the same conditions. Higher photocatalytic activity of Ar400 than P25 was probably caused by its higher surface area and high hydroxylation[5].

EPS spheres with bilayer SiO_2-TiO_2 indicated similar or somewhat lower photocatalytic activity than EPS coated TiO_2. This was probably caused by the inhomogeneous distribution of the titania sample on the P-SiO_2 spheres. In the case of P25, the increase of its coating from 18 to 29 wt% did not cause any improvement in the photocatalytic activity. Most probably TiO_2 coating in P-P25 was thicker than the penetration depth of UV light and higher quantity of the photocatalyst didn't increase its activity.

Effectiveness of the ethylene removal from air for both, stationary and fluidized beds was calculated, taking into

account volume of a treated gas stream and amount of C_2H_4 removed at the time. Firstly, C_2H_4 concentration was expressed in mg/m^3:

$$C\left[{}^{mg}/_{m^3}\right] = \frac{C\,[ppm_v]\cdot M\left[{}^{g}/_{mole}\right]}{V} \quad (5)$$

For 50 ppm$_v$ of ethylene, the following value was obtained:

$$50\ ppm_v = 61.6\ {}^{mg}/_{m^3} = 61.6\cdot 10^{-6}\ {}^{mg}/_{ml} \quad (6)$$

Quantity of C_2H_4 in the volume of a gas stream was related to the volumetric flow rate, according to the following calculations:

$$C\left[{}^{mg}/_{ml}\right] = \frac{m\,[mg]}{V\,[ml]} \quad (7)$$

$$\dot{V}\left[{}^{ml}/_{min}\right] = \frac{V\,[ml]}{t\,[min]} \quad (8)$$

$$\dot{m} = \frac{m}{t} = C\cdot\dot{V} = \frac{m}{V}\cdot\frac{V}{t} \quad (9)$$

where is C_2H_4 concentration, is the volumetric flow rate and is a mass flow rate of C_2H_4 present in air.

For the static bad, by assuming that 100% of the photocatalytic decomposition of C_2H_4 occurs under flow of 20 ml/min and UV irradiation (sample Ar400), the following mass of C_2H_4 decomposition per minute is obtained from the calculations below:

$$\dot{m} = 61.6\cdot 10^{-6}\left[{}^{mg}/_{ml}\right]\cdot 20\left[{}^{ml}/_{min}\right] = \\ = 1.23\cdot 10^{-3}\left[{}^{mg}/_{min}\right] = 1.23\left[{}^{\mu g}/_{min}\right] \quad (10)$$

Similar calculations were performed for the other samples in both conditions of the photocatalytic system, at the stationary and fluidized bed. The results were illustrated in Fig. 8.

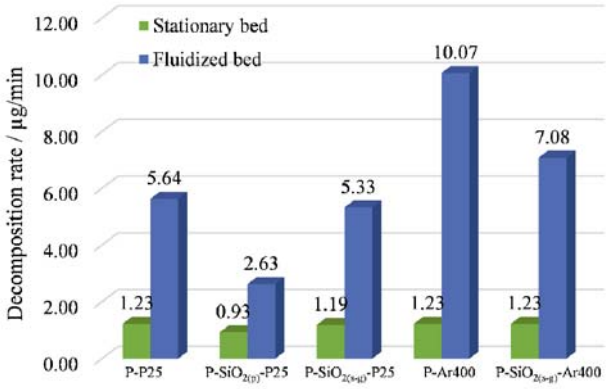

Figure 8. Photocatalytic decomposition rate of C_2H_2 in the reactor with the stationary and fluidized bed expressed in μg/min

Fluidized bed reactor appeared to be much more efficient in ethylene removal than that with the stationary bed. It was caused by the increased speed of C_2H_4 mass transfer to the photocatalyst surface and better utilization of the incident UV light. At the stationary bed, the composites located in the center of the quartz tube probably were not irradiated due to the shielding effect of the spheres present on the edges of tube. In the fluidized bed reactor higher quantity of a contaminated air can be purified during irradiation time than it is in the stationary bed reactor and better utilization of the UV light can be achieved. Measured shielding effect of the stationary bed was around 42–44%, whereas in the fluidized bed was only 28%, due to the increased transparency of the feed.

Importance of the irradiation process in the fluidized bed reactor on the efficiency of the photocatalytic reactions was reported by the other researchers[20]. The optical path length of the emitted light to the photocatalytic bed and its scattering can greatly decide about the yield of ethylene degradation.

CONCLUSIONS

Application of the fluidized bed reactor for the photocatalytic removal of ethylene from the gas stream appeared to be very advantageous for air purification, because the efficiency of the C_2H_4 decomposition rate was around 8 times higher by comparison with the process conducted with the static bed, as shown for sample P-Ar400. Moreover, application the flow rate of 500 ml/min under bed fluidization allows to obtain purification of higher volume of air at time. High efficiency of fluidized bed was caused by better utilization of UV light. The yield of the photocatalytic process depended on the amount and type of TiO_2 material. TiO_2 consisted from anatase phase, which had high surface area and high surface hydroxylation was very active for C_2H_4 degradation. This mentioned TiO_2 showed better affinity towards SiO_2 than commercial TiO_2-P25, what allowed to obtain higher quantity of TiO_2 coating on P-SiO_2 spheres. Prepared photocatalyst bed P-$SiO_{2(s\text{-}g)}$-Ar400 revealed high photocatalytic activity towards ethylene decomposition and stability during fluidization process, however longer period of time is necessary for further studies. Contrary to that EPS coated Ar400 was less stable under fluidization process, probably some parts of TiO_2 peeled away and then the observed rate of ethylene decomposition was slightly decreasing. The proposed preparation and application of P-$SiO_{2(s\text{-}g)}$-Ar400 composite in the fluidized bed reactor seems to be a good solution for the removal of ethylene from air due to its high efficiency, stability and low cost.

ACKNOWLEDGEMENTS

This research was funded by the National Science Centre, Poland, grant nr 2020/39/B/ST8/01514.

LITERATURE CITED

1. Zhu, Z., Zhang, Y., Shang, Y. & Wen, Y. (2019). Electrospun Nanofibers Containing TiO_2 for the Photocatalytic Degradation of Ethylene and Delaying Postharvest Ripening of Bananas. *Food Bioprocess Technol*. 12, 281–287. DOI: 10.1007/s11947-018-2207-1.

2. de Chiara, M.L.V., Pal, S., Licciulli, A., Amodio, M.L. & Colelli, G. (2015) Photocatalytic degradation of ethylene on mesoporous TiO_2/SiO_2 nanocomposites: Effects on the ripening of mature green tomatoes, *Biosystems Engineering* 132, 61–70. DOI: 10.1016/j.biosystemseng.2015.02.008.

3. Keller, N., Ducamp, M.-N., Robert, D. & Keller, V. (2013). Ethylene Removal and Fresh Product Storage: A Challenge at the Frontiers of Chemistry. Toward an Approach by Photocatalytic Oxidation. *Chem. Rev.* 113, 5029–5070. DOI: 10.1021/cr900398v.

4. Maneerat, C., Hayata, Y., Egashira, N., Sakamoto, K., Hamai, Z. & Kuroyanagi, M. (2003). Photocatalytic reaction of TiO_2 to decompose ethylene in fruit and vegetable storage. Transactions of the ASAE 46(3), 725–730. DOI: 10.13031/2013.13574.

5. Rychtowski, P., Tryba, B., Skrzypska, A. & Felczak, P. et al. (2022) Role of the Hydroxyl Groups Coordinated to TiO_2 Surface on the Photocatalytic Decomposition of Ethylene at Different Ambient Conditions. *Catalysts* 12, 386. DOI: 10.3390/catal12040386.

6. Maneerat, C., Hayata, Y. Gas-phase photocatalytic oxidation of ethylene with TiO_2-coated packaging film for horticultural products. (2008). Transactions of the ASABE 51(1), 163–168. DOI: 10.3390/ma12060896.

7. Iwanaga, M., Akimoto, Y. & Shiraishi, F. (2019) Effect of humid air on photocatalytic decomposition of ethylene by TiO_2 immobilized on different supports. *Eco-Engineering* 31(2), 37–44. DOI: 10.11450/seitaikogaku.31.37.

8. de Chiara, M.L.V., Amodio, M.L. Scura, F., Spremulli, L. & Colelli, G. (2014). Design and preliminary test of a fluidised bed photoreactor for ethylene oxidation on mesoporous mixed SiO_2/TiO_2 nanocomposites under UV-A illumination. *J. Agric. Engin.* XLV,435, 146–152. DOI: 10.4081/jae.2014.435.

9. Ji, B., G. Yan, W. Zhao, X. Zhao, J. Ni, , J. Duan, Z. Chen & Z. Yang. (2020). Titanium mesh-supported TiO_2 nano-film for the photocatalytic degradation of ethylene under a UV-LED. *Ceramics International* 46, 20830–20837. DOI: 10.1016/j.ceramint.2020.05.113.

10. Hussain, M., Bensaid, S., Geobaldo, F., Saracco,, G. & Russo N. (2011). Photocatalytic Degradation of Ethylene Emitted by Fruits with TiO_2 Nanoparticles. *Ind. Eng. Chem. Res*. 50, 2536–2543. DOI:10.1021/ie1005756.

11. Park, D.-R., Zhang, J., Ikeue, K., Yamashita, H. & Anpo, M. (1999). Photocatalytic Oxidation of Ethylene to CO_2 and H_2O on Ultrafine Powdered TiO_2 Photocatalysts in the Presence of O_2 and H_2O. *J. Catal.* 185, 114–119. DOI: 10.1006/jcat.1999.2472.

12. Hauchecorne, B., Tytgat, T., Verbruggen, S.W., Hauchecorne, D., et al. (2011). Photocatalytic degradation of ethylene: An FTIR in situ study under atmospheric conditions. *Appl. Catal. B: Environ*. 105(1–2), 111–116. DOI: 10.1016/j.apcatb.2011.03.041.

13. Rychtowski, P., Orlikowski, J., Żołnierkiewicz, G. & Tryba, B. (2022). Mechanism of hydroxyl radicals formation on the reduced rutile. *Mater. Res. Bulletin* 147, 111643. DOI: 10.1016/j.materresbull.2021.111643.

14. Broniarz-Press, L., Agacinski, P., Rozanski, J. (2007). Shear-thinning fluids flow in fixed and fluidised beds. Int. *J. Multiph. Flow*, 33, 675–689. DOI: 10.1016/j.ijmultiphaseflow.2006.12.004.

15. Kuo, H.P., Wu, C.T. & Hsu, R.C. (2011). Continuous toluene vapour photocatalytic deduction in a multi-stage fluidised bed. *Powder Technol.* 210, 225–229. DOI: 10.1016/j.powtec.2011.03.022.

16. Lim, T.H. & Kim, S.D. Photocatalytic degradation of trichloroethylene over TiO_2/SiO_2 in an annulus fluidized bed reactor. (2002). *Korean J. Chem. Eng*. 19, 1072–1077. DOI:10.1007/BF02707235.

17. Tryba, B., Rychtowski, P., Srenscek-Nazzal, J. & Przepiórski, J. (2020). The influence of TiO_2 structure on the complete decomposition of acetaldehyde gas, *Mater. Res. Bulletin* 126, 110816. DOI: 10.1016/j.materresbull.2020.110816.

18. Wu, C.-Y., Tu, K.-J., Deng, J.-P., Lo, Y.-S. & Wu ,C.-H. (2017). Markedly Enhanced Surface Hydroxyl Groups of TiO_2 Nanoparticles with Superior Water-Dispersibility for Photocatalysis. *Materials*, 10, 566. DOI: 10.3390/ma10050566.

19. Chen, W., Takai, C., Khosroshahi, H.R., Fuji, M. & Shirai, T. (2015). Surfactant-free fabrication of SiO_2-coated negatively charged polymer beads and monodisperse hollow SiO_2 particles, Colloids Surfaces A Physicochem. *Eng. Asp*. 481, 375–383. DOI:10.1016/j.colsurfa.2015.06.008.

20. Ciambelli, P., Sannino, D., Palma, V., Vaiano, V. & Mazzei, R. S. (2009). Improved Performances of a Fluidized Bed Photoreactor by a Microscale Illumination System. Internat. J. Photoenergy, 2009, Article ID 709365. DOI: 10.1155/2009/709365.